

FLUID PROPULSION IN MICRO-CHANNELS USING MAGNETICALLY-ACTUATED ARTIFICIAL CILIA: A BIO-MIMETIC APPROACH

Syed Khaderi¹, Michiel Baltussen², Patrick Anderson², Daniel Ioan³, Jaap den Toonder² and
Patrick Onck^{1*}

¹Zernike Institute for Advanced Materials, University of Groningen, Groningen, The Netherlands,

²Eindhoven University of Technology, Eindhoven, The Netherlands,

³"POLITEHNICA" University of Bucharest, Bucharest, Romania

s.n.khaderi@rug.nl, m.g.h.m.Baltussen@tue.nl, p.d.anderson@tue.nl, lmn@lmn.pub.ro,

jaap.den.toonder@philips.com, p.r.onck@rug.nl

KEY WORDS

Artificial cilia, metachronal wave, magnetic actuators

ABSTRACT

A micron-scale fluid propulsion that occurs in nature uses oscillating hair-like structures called cilia. They move such that they rigidly rotate about their fixed base for the first half of the cycle and come back to their initial position with a whip-like motion during the second half. In addition to this, every cilium beats with a phase difference with its neighbour, thereby generating metachronal waves. In this work we design super-paramagnetic artificial cilia which can mimic the motion of natural cilia when actuated using a suitable magnetic field. We study how the flow generated by these artificial cilia in a channel depends on their lateral spacing. Furthermore, we study the effect of the metachronal wave on the generated flow. We show that the flow created in the presence of a metachronal wave is larger than the flow created by synchronously moving cilia, becoming maximal in case of antiplectic metachrony.

1. INTRODUCTION

One of the key challenges in the rapidly growing field of lab-on-a-chip is to transport fluids through channels at micron-scale dimensions. The fluid transport in micro-channels is often performed by downscaling conventional methods such as syringe pumps, micropumps, or by exploiting electro-magnetic fluid manipulation principles, as in electro-osmotic and magneto-hydrodynamic devices. In search for novel ways to propel fluids at micron scales, we let nature be our guide. Nature uses hair-like structures called cilia, which are attached to the surfaces of micro-organisms to propel fluids at small length scales, and therefore they swim. The typical length of a cilium is 10 microns. These hair-like structures beat or move in a whip-like asymmetric manner consisting of an effective stroke and recovery stroke. Moreover, when many cilia operate together, they beat with a constant phase-lag with their neighbors. This leads to the formation of metachronal waves, which are known to enhance the fluid flow due to cilia. The asymmetric motion of natural cilia is due to the intricate interaction between the cilia microstructure and the internally actuating motor-protein dynein. It is a challenging task to design the artificial counterpart of cilia, which are actuated by external force fields and mimic their asymmetric motion.

In this work, we design artificial cilia using polymer films with embedded magnetic nano-particles. Tapered super-paramagnetic (SPM) polymer films mimic the asymmetric motion of natural cilia when subjected to a

*Corresponding author

rotating magnetic field. By coupling magnetostatic field equations to computational solid mechanics and computational fluid dynamic models we verify whether the asymmetric motion of the SPM cilia creates any fluid flow. Furthermore, we study how the generated flow depends on the spacing between the cilia and the height of the channel. Finally, we study the effect of metachronism on an array of cilia and demonstrate that the flow created in the presence of metachronism is larger than the flow created when the cilia are beating synchronously.

Attempts have been made in the past to model the fluid flow induced by ciliary motion using the envelope model [3, 1], the sublayer model [2, 8, 12, 7], fluid structure interaction models with the lattice-Boltzmann approach [10] and the immersed boundary method [4]. Recently, three dimensional motion of magnetic cilia was shown to be able to propel fluids in microchannels [5]. However, the dependence of the volume of the fluid transported as a function of cilia spacing, the wavelength of the metachronal wave and its direction (symplectic or antiplectic metachrony) and channel dimensions has not been fully documented until now.

2. COMPUTATIONAL MODEL

We discretize the cilia using Euler-Bernoulli beam elements taking into consideration the geometric non-linearity and the inertia of the cilia [9]. The magnetic field is calculated by solving the Maxwell's equations using a boundary element approach. The Stokes equation, which captures the behavior of the fluid flow at low Reynolds numbers, is solved for the velocity and pressure using finite elements. The velocity is interpolated quadratically, while the pressure is interpolated linearly within each element. The solid-fluid coupling is performed by imposing that the velocity of the cilia is equal to the velocity of the fluid. This condition is enforced at the nodal points of the Euler-Bernoulli beam elements using Lagrange multipliers (point collocation method), within a fictitious domain framework [14]. The solution procedure is as follows. The Maxwell's equations are solved at every time instant to solve for the magnetic field. From the magnetic field, we calculate the magnetic body couple acting on the cilia. This body couple acting on cilia is given as an input to the implicitly-coupled solid-fluid model, which simultaneously solves for the cilia velocity, and velocity and pressure of the fluid. The velocity of the cilia is integrated using Newmark's algorithm to calculate its new position, and this procedure is repeated, see [9]. A fixed time-step of $1 \mu\text{s}$ is used during the simulations. The streamlines are obtained from the velocity field in the fluid using the visualization software Tecplot [13].

3. RESULTS

3.1 Asymmetric motion of super-paramagnetic cilia

We study a periodic arrangement of super-paramagnetic (SPM) cilia in a microfluidic channel of height H , with the cilia spaced a apart. A unit-cell is defined that contains one cilium. No-slip boundary conditions are applied at the top and bottom boundaries of the channel and periodic boundary conditions at the left and right ends of the unit-cell. The fluid has a viscosity $\mu = 1 \text{ mPas}$. A straight, magnetically anisotropic SPM film (having susceptibilities 4.6 and 0.8 in the tangential and normal directions [15], respectively), is subjected to a magnetic field with magnitude $B_0 = 31.5 \text{ mT}$ that is pointing initially along the length of the cilium, and then rotated from 0° to 180° in $t = 10 \text{ ms}$ and then kept constant during the rest of the cycle. The film has a length $L = 100 \mu\text{m}$, effective elastic modulus $E = 1 \text{ MPa}$ and density $\rho = 1600 \text{ kg/m}^3$. Its cross-section is tapered, with the thickness varying linearly along its length, having $h = 2 \mu\text{m}$ at the left (attached to the substrate) end and $h = 1 \mu\text{m}$ at the right end. Figure 1(a) shows that in the effective stroke the portion of the beam near the free end is nearly straight. This is due to the fact that in this region the film can easily follow the rotating applied field so that field and magnetization remain almost parallel, causing the magnetic torque to be low in this region of the film (instances 2, 3 and 4 in Fig. 1(b)). When the film has reached position 4, the magnetization in the film is such that the torques are oriented clockwise near the fixed end and anticlockwise near the free end, resulting in strong bending of the film. From Fig. 1(b) it can be seen that during the recovery stroke (in black) the position of zero torque propagates from the fixed end to the free end (from instance 4 to 5). Here the tapering is essential, causing the torque per unit length to be higher at the fixed end, allowing the film to recover to the initial position (1). This behavior is very similar to that of natural cilia [11]. The motion of the cilium is strongly asymmetric, and the tip of the cilium traces a closed contour that defines a swept area. It is to be noted that the film recovers in the presence of an applied magnetic field. This sensitive interplay between

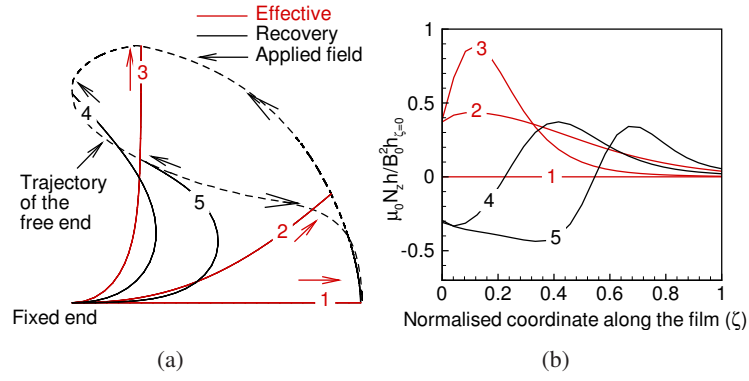


Figure 1: Motion of a super-paramagnetic (SPM) cilium in a rotating magnetic field, during the propulsion of fluid. (a) Snapshots of the cilium at 0 ms, 2.5 ms, 5.0 ms, 7.5 ms and 8.5 ms. (b) Normalized torque distribution along the film corresponding to the snapshots shown in (a). Here μ_0 is the permeability of vacuum, h is the thickness at position ζ and $h_{\zeta=0}$ is the thickness at the fixed end.

stored elastic energy and controlled magnetic field can be exploited to provide a large asymmetry in motion.

3.2 Fluid flow

Next, we analyze how much fluid is propelled by the super-paramagnetic artificial cilia. The velocity field at different instances of time for a SPM cilium for $H/L = 2$ and $a/L = 2$ is shown in Fig. 2. The pumping action can be nicely seen when we observe the motion of fluid particles due to the motion of the cilium. The fluid particles are represented by solid black circles in Fig. 2. As the cilium moves during the effective and the recovery stroke, the fluid particles are dragged back and forth. Due to the asymmetric motion of the film, we see a difference between the initial and final position of particles. The fluid particles have thus obtained a net displacement to the left (see Fig. 2). It is to be noted that the fluid flow is fluctuating in nature.

3.3 Effect of cilia spacing and channel height

The normalised area flow (area flow/ $(\pi L^2/2)$) as a function of the cilia spacing \hat{a}/L for various channel heights H/L is shown in Fig. 3(a). It can be seen that the area flow decreases as the cilia spacing is increased. There can be two reasons for the decrease in the flow. Firstly, a decrease in the swept area can decrease the area flux. Secondly, when the cilia spacing is increased the fluid drag forces increase and thus the area flux gets reduced. As the SPM cilia is subjected to a rotating magnetic field, its velocity is nicely controlled. Hence the film sweeps approximately the same area for all cilia spacings. This can be observed when we see the trajectory of the free end of the film as the spacing is increased, Fig. 3(b). In fact, it can be seen from Fig. 3 that the swept area shows a minor decrease for small a/L . Hence, the reduction in the area flow (as we increase the spacing) is only due to increased fluid viscous forces, due to the larger cilia spacing.

For a given a/L , the flux increases linearly with H/L . The reason for this can be understood from the velocity contours and the respective velocity profile at the boundary, see Fig. 4. The maximum velocity occurs at the free end of the film and zero at the bottom and the top of the channel. As H/L is increased the velocity profile becomes nearly linear at the inlet/exit of the channel from $y = L$ to $y = H$. Hence, the area flow increases as H/L is increased, see Fig. 3(a).

3.4 Out-of-phase motion of cilia

We study the flow created due to an two-dimensional array of magnetic artificial cilia, with spacing a , which are actuated using a non-uniform magnetic field, in the limit where the inertia effects in the fluid are negligible ($Re \approx 0$). The applied external magnetic field varies in space and time such that

$$B_x = B_0 \cos(\omega t - 2\pi x/\lambda) \quad B_y = B_0 \sin(\omega t - 2\pi x/\lambda).$$

The applied magnetic field travels in space and time with a velocity $\lambda\omega$, where λ is the wave length of the non-uniform magnetic field and $\omega = 2\pi/t_{\text{ref}}$ is the angular frequency and t_{ref} is the cycle time. The time and

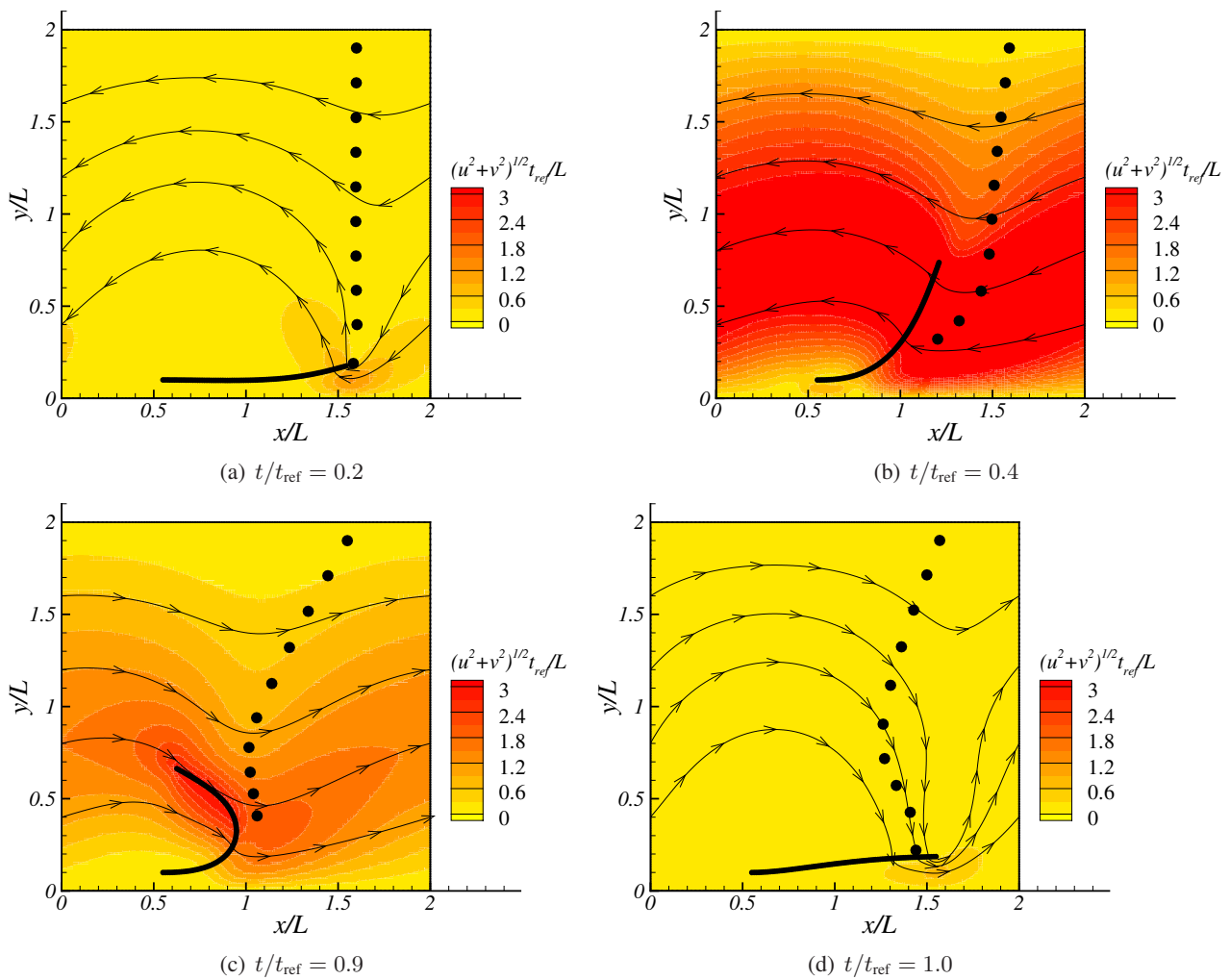


Figure 2: Velocity field and streamlines at different time instances for a SPM film for $H/L = 2$, $a/L = 2$. The solid black circles at different instances represent the position of fluid particles which formed initially a straight vertical line.

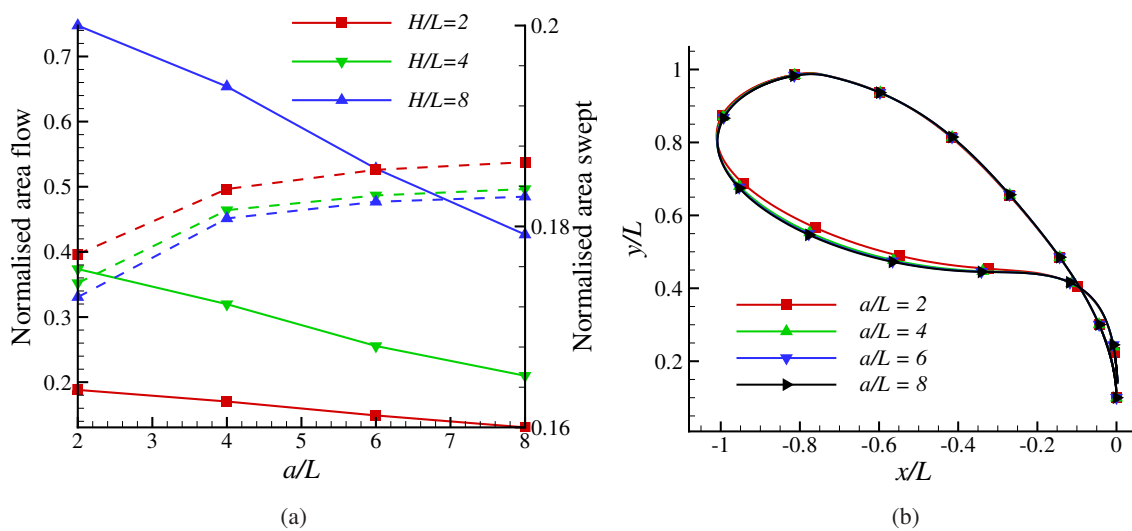


Figure 3: (a) Area flow as a function of geometry. Solid lines represent the normalised area flow out of the channel and the broken lines represent the area swept by the cilium. (b) Trajectory of the free end of the SPM cilia for various cilia spacings.

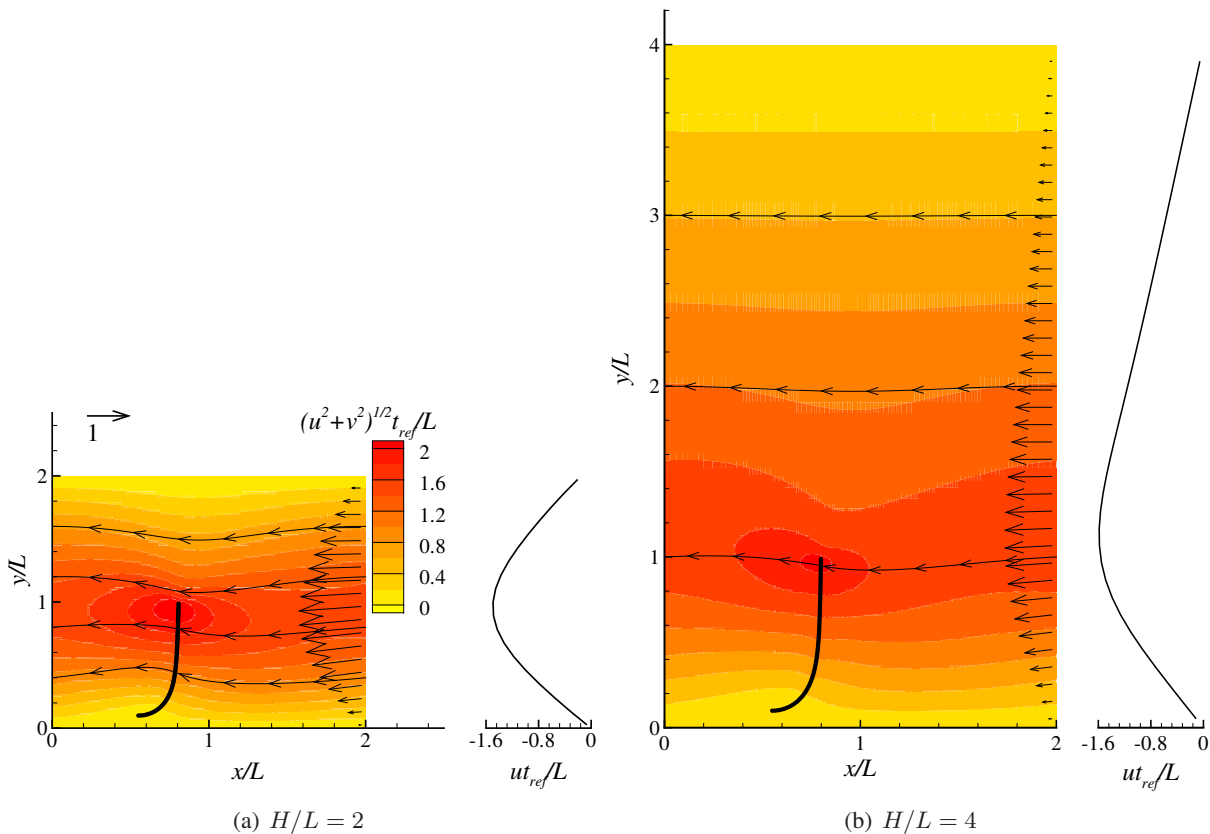


Figure 4: Velocity profiles at 5 ms for $a/L = 2$. Variation of the horizontal component of velocity at the periodic boundary along the height of the channel is plotted next to the respective velocity profile. The maximum velocity occurs at the free end of the film and zero at top substrate and top of the channel. As H/L is increased, the velocity profile becomes nearly linear at the exit of the channel. Hence the area flow increases as H/L is increased, see Fig. 3(a).

space variation of the magnetic field, for example, can be achieved by using current wires embedded in microchannels[6]. The fluid flow is characterised by two parameters: the net volume of the fluid transported during one cycle and the effectiveness. The cilium pushes the fluid forward during the effective stroke, creating a ‘positive area flow’ Q_p in the direction of the effective stroke and pushes the fluid back during the recovery stroke creating a ‘negative area flow’ Q_n . Due to the asymmetric motion, the positive flow is larger than the negative flow, generating a positive area flow per cycle ($Q_p - Q_n$). The effectiveness, defined as $(Q_p - Q_n)/(Q_p + Q_n)$, indicates which part of the totally displaced fluid is effectively converted into a net flow. An effectiveness of unity represents a unidirectional flow.

The fluid propelled and the corresponding effectiveness is plotted for different ratios of cilia spacing a to the wavelength λ , see Fig. 5. When all the cilia are moving synchronously ($a/\lambda = 0$ or $1/2$), the flow created will be the same as the flow created by one cilium kept in a periodic unit-cell. Now, as the cilia spacing is decreased from $a = 5L$ to $a = 2.5L$, the viscous resistance decreases which increases the fluid flow. As the cilia density is further increased to $a = 1.67L$, the cilia start interacting with each other and fluid flow does not show an increase any further. Also, when $a/\lambda = 0$ or 0.5 , the effectiveness of fluid propulsion is very low (Fig. 5(b)). The fluid flow and the effectiveness show an increase once the cilia start moving with a phase lag between each other. The fluid flow remains constant for all wavelengths when the inter-cilium spacing is large ($a = 5L, 2.5L$). When the cilia spacing is low, e. g. for $a = 1.67L$ we see a larger increase in the fluid flow when there is an antiplectic metachrony compared to the flow when there is a symplectic metachrony. This is due to the hydrodynamic interaction between adjacent cilia.

The interaction between the cilia for small inter-cilium spacing can be understood when we look at the velocity field corresponding to the symplectic and antiplectic metachrony for the same wave speed (12ω cilia per second) when the third cilium from the left is exhibiting the recovery stroke, as shown in Fig. 6. The

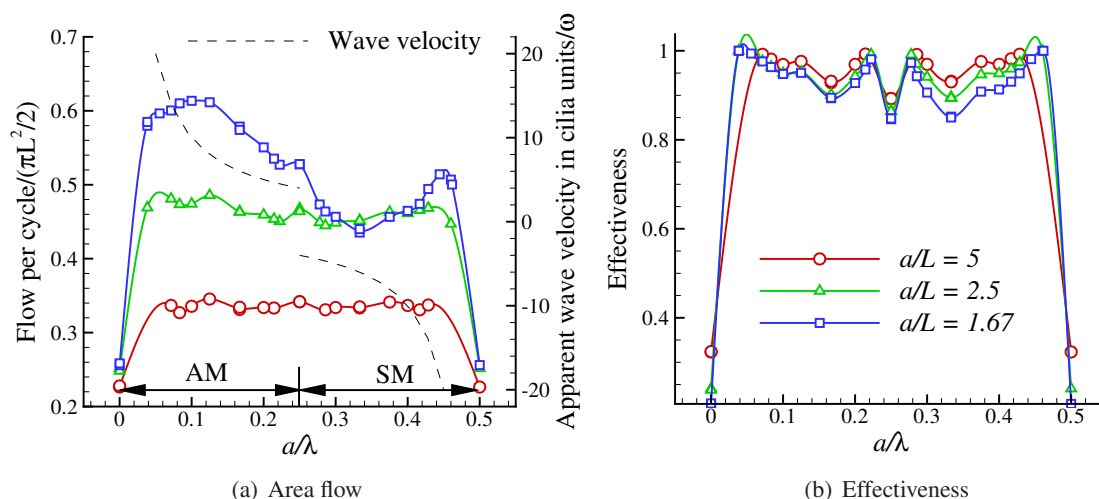


Figure 5: Flow and effectiveness as a function of a/λ for different inter-cilium spacings. AM and SM refer to antiplectic metachrony (the wave direction is opposite to the direction of the effective stroke) and symplectic metachrony (the wave direction and the effective stroke direction are same), respectively.

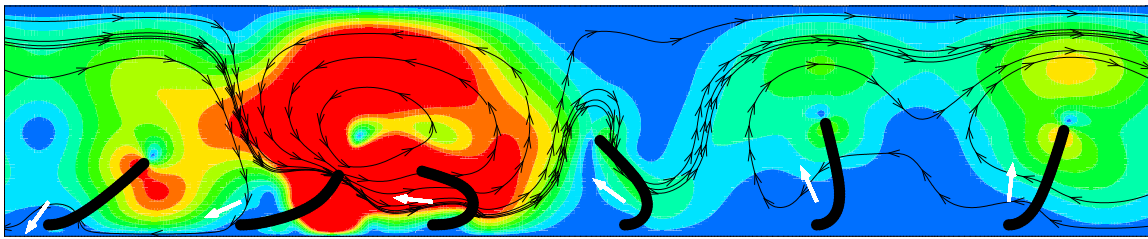
second and third cilia from the left are in the recovery stroke for the antiplectic metachrony. For the symplectic metachrony the third and fourth cilia from the left are in the recovery stroke. In the case of antiplectic metachrony, the negative flow created by the second and the third cilium from the left is obstructed by the upright position of the fourth cilium, which is about to begin its recovery stroke. As a result, we observe the formation of a vortex with only a small amount of fluid flow in the negative direction. In the case of symplectic metachrony, the position of the fifth cilium from the left is such that the negative flow created by the third and fourth cilium from the left is not resisted. This leads to a larger fluid flow in the negative direction. Moreover, in the case of symplectic metachrony, flow due to the recovery stroke of the fourth cilium from the left resists the effective stroke of the fifth cilium; whereas in the case of antiplectic metachrony, the recovery stroke of the second and the third cilia from the left helps the fourth cilia during its recovery stroke. Therefore, the flow created by an antiplectic metachrony is higher than the flow created by its symplectic counterpart. When the cilia are not interacting with each other through the flow field (example $a = 5\lambda$), the flow generated remains (approximately) constant for all apparent wave speeds.

4. CONCLUSION

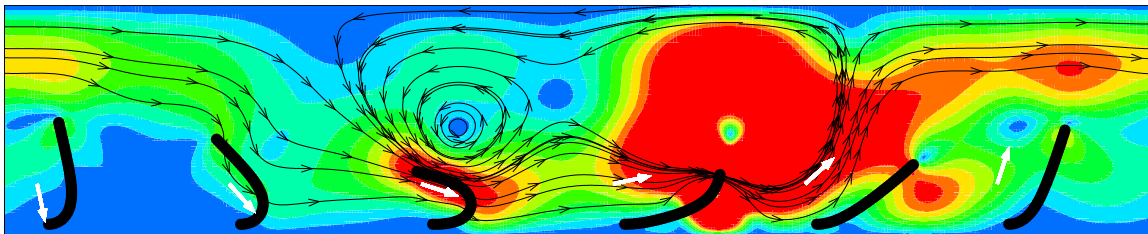
We have shown that a tapered super-paramagnetic film subjected to a rotating magnetic field can exhibit a strong asymmetric motion. With the use of particle tracking, we have verified that this asymmetric motion can generate a modest flow with large fluctuation. The cilia can generate a flow of $60 \mu\text{l}/\text{min}$ (assuming the channel width is 5 mm). This flow increases when we either decrease the cilia spacing or increase the channel height. The flow per cycle and the effectiveness are enhanced as soon as the cilia start to beat with a phase difference. The amount of enhancement in the flow depends on the inter-cilia spacing. However, the effectiveness (which is a measure of the unidirectionality of flow) is not significantly influenced by the spacing of cilia. Interestingly, we find that the enhancement is achieved even at large wavelength (with only small phase lag between adjacent cilia). The direction of travel of the metachronal wave is important only for small cilia spacing. For such cases, the flow is large when the metachronal wave travels in a direction opposite to the effective stroke (antiplectic metachrony).

ACKNOWLEDGMENTS

This work is a part of the 6th Framework European project ‘Artic’, under contract STRP 033274.



(a) Antiplectic metachrony: wave travels to the right



(b) Symplectic metachrony: wave travels to the left

Figure 6: Snap shots for symplectic and antiplectic metachrony for $a/\lambda = 1/12$. The contours represent the absolute velocity normalised with L/t_{ref} (blue and red colours represent a velocity of 0 and 2, respectively). The direction of the velocity is represented by streamlines. The applied magnetic field is shown by the white arrows.

REFERENCES

- [1] J. R. Blake. Infinite models for ciliary propulsion. *Journal of Fluid Mechanics*, 49(02):209–222, 1971.
- [2] J. R. Blake. A model for the micro-structure in ciliated organisms. *Journal of Fluid Mechanics*, 55(01):1–23, 1972.
- [3] Christopher Brennen and Howard Winet. Fluid mechanics of propulsion by cilia and flagella. *Annual Review of Fluid Mechanics*, 9:339–398, 1977.
- [4] A. Dauptain, J. Favier, and A. Bottaro. Hydrodynamics of ciliary propulsion. *Journal of Fluids and Structures*, 24(8):1156 – 1165, 2008. Unsteady Separated Flows and their Control.
- [5] M. T. Downton and H. Stark. Beating kinematics of magnetically actuated cilia. *EPL (Europhysics Letters)*, 85(4):44002, 2009.
- [6] F. Fahrni. *Magnetic polymer actuators for microfluidics*. PhD thesis, Eindhoven University of Technology, 2008.
- [7] E. M. Gauger, M. T. Downton, and H. Stark. Fluid transport at low Reynolds number with magnetically actuated artificial cilia. *The European Physical Journal E*, 28:231–242, 2009.
- [8] S. Gueron, K. Levit-Gurevich, N. Liron, and J. J. Blum. Cilia internal mechanism and metachronal coordination as the result of hydrodynamical coupling. *Proceedings of the National Academy of Sciences of the United States of America*, 94(12):6001–6006, 1997.
- [9] S. N. Khaderi, M. G. H. M. Baltussen, P. D. Anderson, D. Ioan, J. M. J. den Toonder, and P. R. Onck. Nature-inspired microfluidic propulsion using magnetic actuation. *Physical Review E*, 79(4):046304, 2009.
- [10] Y. W. Kim and R. R. Netz. Pumping fluids with periodically beating grafted elastic filaments. *Physical Review Letters*, 96(15):158101, 2006.
- [11] M. Murase. *Dynamics of cellular motility*. John Wiley and Sons, 1992.
- [12] D. J. Smith, E. A. Gaffney, and J. R. Blake. Discrete cilia modelling with singularity distributions: Application to the embryonic node and the airway surface liquid. *Bulletin of Mathematical Biology*, 69:1477–1510, 2007.
- [13] Tecplot, 2008. Tec360 user manual.
- [14] R. van Loon, P. D. Anderson, and F. N. van de Vosse. A fluid-structure interaction method with solid-rigid contact for heart valve dynamics. *Journal of Computational Physics*, 217:806–823, 2006.
- [15] L. van Rijsewijk. Electrostatic and magnetic microactuation of polymer structures for fluid transport. Master’s thesis, Eindhoven University of Technology, 2006.